Combined facile methods of the DSC and origin lab program to study the dehydration kinetics of KMnPO$_4$·H$_2$O

Chanaiporn Danvirutai · Pittayagorn Noisong

Abstract Thermal dehydration kinetics of potassium manganese phosphate monohydrate (KMnPO$_4$·H$_2$O) was studied using alternative procedure, including the combination between DSC data and Origin Lab program. The results revealed that this convenient method is a suitable tool for the determination of reliable kinetic parameters. The peak area at current temperature can be calculated using the Origin Lab program. Consequently, the kinetic parameters by non-isothermal equations can be calculated. The apparent activation energies were found to be 101.26 and 101.45 kJ mol^{-1} using KAS and iterative methods, respectively. The natural logarithms of pre-exponential factor (lnA) were found to be 12.2775 and 12.4157, respectively based on mechanism function of $g(\alpha) = (1 - (1 - \alpha)^{2/3})$. The experimental enthalpy change of the dehydration process of the studied compound was about 290 J g^{-1}. All detectable peaks from XRD patterns of this compound are indexed as the formula KMnPO$_4$·H$_2$O according to the standard data file PDF#802360. The SEM micrograph exhibits the loose agglomeration phenomenon among the thin plate, which supports the existence of the layered structure compound.

C. Danvirutai · P. Noisong (✉)
Department of Chemistry, Faculty of Science, Materials Chemistry Research Center, Khon Kaen University, Khon Kaen 40002, Thailand
e-mail: pittayagorn@kku.ac.th

C. Danvirutai
e-mail: chanai@kku.ac.th

C. Danvirutai
Department of Chemistry and Center of Excellence for Innovation in Chemistry, Faculty of Science, Khon Kaen University, Khon Kaen 40002, Thailand

Introduction

The KMnPO$_4$·H$_2$O is known to be isostructural with Dittmaite compound (NH$_4$MgPO$_4$·H$_2$O) [1], which is used in various applications such as fireproof material, fertilizer, pigment for paints, furnishes for protection of metals, and for extraction of divalent cations from seawater [2–4]. Now a days, this compound can be used as the important precursor for the synthesis of LiMnPO$_4$ [LiMPO$_4$ (M = Fe, Mn, Co, Ni), Olivine compounds] via cation exchange pathway [5]. These compounds are being actively investigated and have been considered as one of the most promising cathode materials for lithium ion batteries because of their properties of low cost, environmental benign, higher thermal stability, abundant availability, and high theoretical specific capacity [6–8]. Unfortunately, little publications are available about the title compound such as studying about pathway of synthesis process [9], vibrational properties [10], and magnetic properties [11]. Therefore, this compound is of current interested. Especially, the development of new synthetic route of nanocrystalline KMnPO$_4$·H$_2$O for using as the precursor for the synthesized LiMnPO$_4$. Moreover, the kinetic property is also of great importance. The main goal of the kinetic study is to determine the process involved in the transformation, interested reaction rate and reaction mechanism in order to understand the structure and property relationship [12].

Both differential scanning calorimetry (DSC) and thermo gravimetric analysis (TG) are known to be excellent methods to study kinetics of solid state reaction under non-isothermal condition [6, 13–18]. Especially, DSC

instrument possesses various advantages such as (i) the DSC cell can be performed as a mini reactor with negligible heat dissipation, able to evaluate with high accuracy both degree of conversion and the reaction rate. (ii) the DSC method provides the variables needed for the solving the heat/mass transfer problems of real processes—heat flow and heat accumulation [16]. Small sample masses are needed as well as the method is simple, versatile, and easy to evaluate the data. However, the DSC instrument is limited for not being used to study the kinetic behavior by various methods except Kissinger method [19], if the peak area at current temperature program cannot be evaluated, which is the weak point of the DSC instrument. Therefore, the search for the alternative tool for solving this problem is of great interest. Hence, this work presents the method by combining the Orgin Lab program and DSC data to study the dehydration kinetics of $KMnPO_4 \cdot H_2O$ in a more advantageous way.

In this work, we demonstrate a modified method (combination of Orgin Lab program and DSC methods) to evaluate the kinetic parameters of the dehydration of $KMnPO_4 \cdot H_2O$ using Kissinger–Akahira–Sunose (KAS) [19, 20] method due to its simple approach to calculate the exact value of activation energy for the single-step dehydration process. However, the iterative method is necessary to determine the reliable or exact activation energy values and the mechanism function. In addition, the synthesized compound was characterized by TG/DTG/DTA, Fourier transform infrared spectroscopy (FTIR), Atomic absorption/Atomic emission spectroscopy (AAS/AES), and X-ray diffraction (XRD). Besides, the morphology was studied by scanning electron microscope (SEM).

Experimental

Preparation and characterization

The $KMnPO_4 \cdot H_2O$ was synthesized using modified method from the literature [21]. An excess amount of saturated K_2HPO_4 (15–20 M) as a potassium and phosphate source was added into 25 mL of 0.5 M $MnCl_2 \cdot 4H_2O$ and 10 mL of acetone mixture, then digested for 24 h. The metal and water contents of synthesized hydrate samples were confirmed using atomic absorption spectrophotometry (AAS/AES, Perkin Elmer, Analyst 100) and TG/DTG/DTA (Perkin Elmer, Pyris Diamond), respectively. The title compound was characterized by FTIR (FTIR/FT Raman spectrophotometer, Perkin Elmer Spectrum GX) and XRD techniques (D8 Advanced powder diffractometer, Bruker AXS, Karlsruhe, Germany) with Cu Kα radiation ($\lambda = 0.15406$ Å) at a current of 30 mA and a voltage of 40 kV and the 2θ value range of 10–70°. The Scherrer equation was used to evaluate the crystallite sizes

(i.e., D $= K\lambda/\beta\cos\theta$, where λ is the wavelength of X-ray radiation, K is a constant taken as 0.89, θ is the diffraction angle, and β is the full width at half maximum). The morphology was studied by SEM instrument (Leo 1450VP) after gold coating.

Differential scanning calorimetry (DSC)

Differential scanning calorimetry (DSC, Perkin Elmer Pyris 1) was used for kinetic studies under non-isothermal condition. The instrument was calibrated for the temperature and enthalpy using an indium prior to perform the investigations. The heating rates were 5, 10, 15, 20, and 25 K min^{-1} and the samples were weighed accurately and sealed in aluminum pans. The sample weight was kept in the range of 4.4–4.6 mg. These DSC scans were recorded from 60 to 350 °C under nitrogen atmosphere with the constant pressure of 20 psi.

Kinetic study by non-isothermal method using Origin Lab Program

Non-isothermal kinetic study using the reaction rate of solid state reaction can be described as the functions of $k(T)$ and $f(\alpha)$:

$$\frac{d\alpha}{dt} = k(T)f(\alpha), \tag{1}$$

where a function $f(\alpha)$ depends on the particular decomposition mechanism, k is the rate constant, t is time, and α is degree of conversion:

$$\alpha = \frac{(m_i - m_t)}{(m_i - m_f)}, \tag{2}$$

where m_i, m_t, and m_f are the initial, current at temperature T, and final mass temperature at which the mass loss is approximately unchanged, respectively.

Upon the substitution of Arrhenius' equation as Eq. 3 into Eq. 1 leads to Eq. 4.

$$k(T) = Ae^{-\frac{E}{RT}}, \tag{3}$$

$$\frac{d\alpha}{dt} = Af(\alpha)e^{-\frac{E}{RT}}. \tag{4}$$

When β is the heating rate ($\beta = dT/dt$, K min^{-1}), Eq. 4 may be written as

$$\frac{d\alpha}{dt} = \frac{dT}{dt}\frac{d\alpha}{dT} = \beta\frac{d\alpha}{dT} = Af(\alpha)e^{-\frac{E}{RT}}. \tag{5}$$

The pre-exponential factor A (min^{-1}), which is assumed to be independent of temperature (T/K), E is the activation energy (kJ mol^{-1}), and R is the gas constant (8.314 J mol^{-1} K^{-1}). The degree of conversion α those collected from the DSC data can be generally expressed as

$$\alpha = \left(\frac{\Delta H_T}{\Delta H_t} \right), \tag{6}$$

where ΔH_T is the peak area equivalent to the heat involved in heating up to the temperature T. ΔH_t is the total peak area equivalent to the heat of transformation and can be determined by combining DSC data and Origin Lab program. The procedure will be described in the results and discussion part.

The KAS equation as one of the most important equation has been used extensively due to its convenient property. This equation was used to determine the activation energy relating to α, E as shown in Eq. 7. All parameters are the same as given in Eq. 5.

$$\ln \frac{\beta}{T^2} = \ln \frac{AE}{g(\alpha)R} - \frac{E}{RT}. \tag{7}$$

The Arrhenius parameters, together with the reaction model, are sometimes called the kinetic triplet. As a consequence of the rearrangement of Eq. 5 followed by integration, obtain $g(\alpha) = \int_0^\alpha \frac{d\alpha}{f(\alpha)}$, is the integral form of the $f(\alpha)$, which is the reaction model that depends on the reaction mechanism. According to Eq. 7, the slopes of the plots of $\ln(\beta/T^2)$ versus $1,000/T$ with better linear correlation coefficient (r^2) lead to the calculation of activation energy values E and pre-exponential factor A. The activation energy values were calculated at the heating rates of 5, 10, 15, 20, and 25 K min^{-1}. The A values were calculated based on the $F_{2/3}$ model of the mechanism upon dehydration of the title compound [22].

Results and discussion

TG/DTG/DTA, FTIR, XRD and SEM

The Mn^{2+} and K^{+} contents of the studied compound were determined by AAS and AES methods, respectively, and the results confirmed 1 mol of metals per formula. TG/DTG/DTA curves of KMnPO$_4\cdot$H$_2$O (Fig. 1) exhibit only one step of mass loss which corresponds to the dehydration process over the temperature range 100–220 °C with the maximum at 197.6 °C. This result agrees with those reported in the literatures [5, 9, 22]. The corresponding observed mass loss is 10.03 %, which agrees with the theoretical mass loss of 8.74 %. The difference % mass loss was due to using high heating rate of 20 K min^{-1}, which is usually 10 K min^{-1}. The DTA curve illustrates the dehydration process with endothermic peak at 201.5 °C. The water molecules, those were eliminated at about 200 °C and above indicate their coordination by the metal cations, while those eliminated at lower temperatures can be either coordinately linked
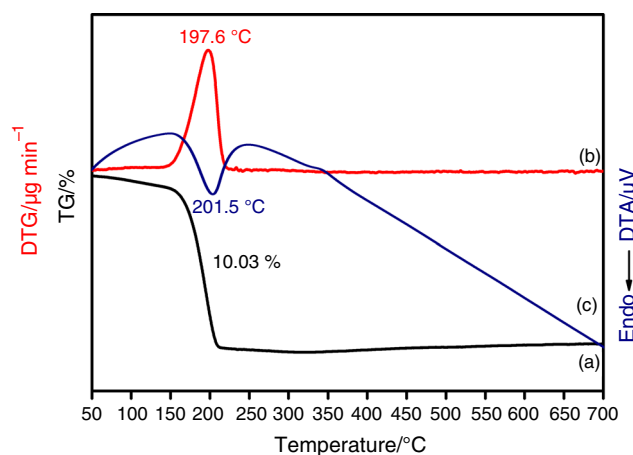

Fig. 1 TG (*a*), DTG (*b*), DTA (*c*) curves of the synthesized KMnPO$_4\cdot$H$_2$O at the heating rates of 20 K min^{-1} in dried air atmosphere

water or water of crystallization [23]. The water molecules in the studied hydrate can be considered to be coordinately linked water as well as water of crystallization.

The broad band in the 3,481–3,223 cm^{-1} region (Fig. 2) can be assigned to symmetric (ν_1) and asymmetric (ν_3) OH stretching vibration of water. The band due to bending vibration ν_2 mode of water molecule was observed around 1,652 cm^{-1}. An interesting observation is the new band at around 1,422 cm^{-1} [24–26]. The lowering of the water bending frequency can be suggested to be due to water–cation interactions with a tendency to be more pronounced when the cation size is small and its charge density is high. This reason was suggested by Falk [27]. The phosphate ion vibrations are found in the ranges of 1,008–931, 500–375,
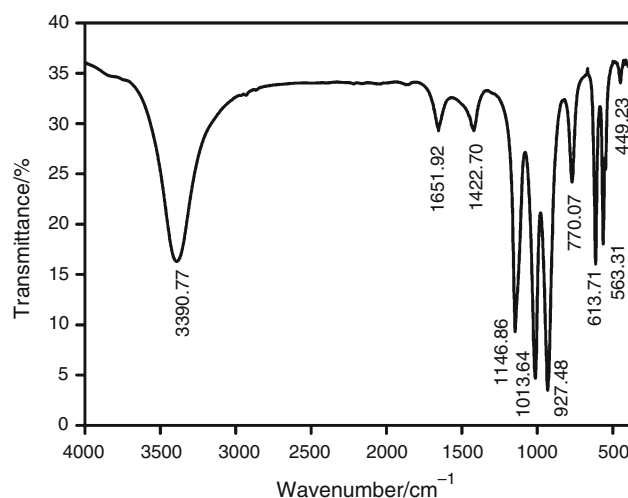

Fig. 2 FTIR spectrum of the synthesized KMnPO$_4\cdot$H$_2$O using KBr press technique

1,176–1,015, and 630–510 cm^{-1} those are assigned to symmetric stretching (v_1), symmetric bending (v_2), asymmetric stretching (v_3), and asymmetric bending (v_4), respectively.

All detectable peaks of the XRD pattern in Fig. 3a are indexed as the formula KMnPO$_4$·H$_2$O structure, those are identified using the standard data of PDF# 802360 (Fig. 3b) and indicate the high crystallinity, which crystallizes in the orthorhombic space group Pmn2$_1$ (a = 5.676, b = 8.335, c = 4.905 Å). The calculated average crystallite size from Scherrer equation was found to be 34.57 nm. The SEM micrograph of this compound is shown in Fig. 4, which shows the thin plate-like morphologies as observed by Koleva [5] and having sizes of about 1.00–2.00 μm in width and 3.00–4.50 μm in length. There is loose agglomeration phenomenon among the thin plate particles, which is considered to indicate the existence of layered structure [9, 10].

DSC and kinetic study

Figure 5 shows the DSC curves at the heating rates of 5, 10, 15, 20, and 25 K min^{-1}. The maximum of the curves shifted to higher temperature as the heating rate increased. The DSC data were evaluated using the Origin Lab program. The determination of the kinetic parameters was carried out according to the following processes: (i) the α values at the heating rate of 5 K min^{-1} were collected from the DSC data in order to calculate the ΔH_T and ΔH_t as described in Eq. 5 by Origin Lab program. (ii) Repeat step (i), but using DSC data at the heating rates of 10, 15, 20, and 25 K min^{-1} instead of those from 5 K min^{-1}. The α–T relation is obtained as shown in Fig. 6 for the heating rate of 5 K min^{-1}. (iii) Using data at step (ii) to calculate the
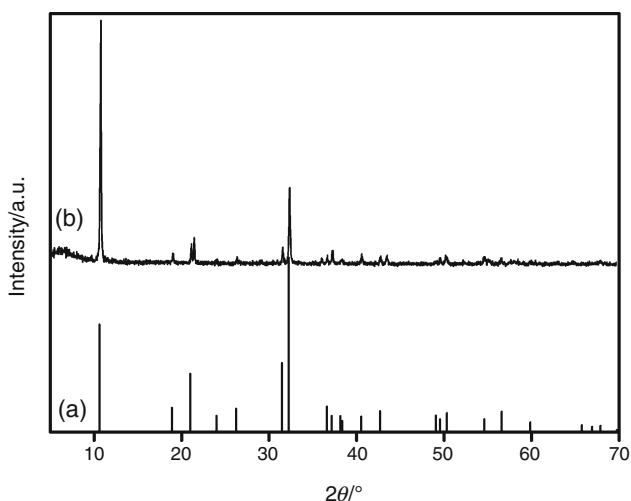

Fig. 4 SEM micrograph of the synthesized KMnPO$_4$·H$_2$O
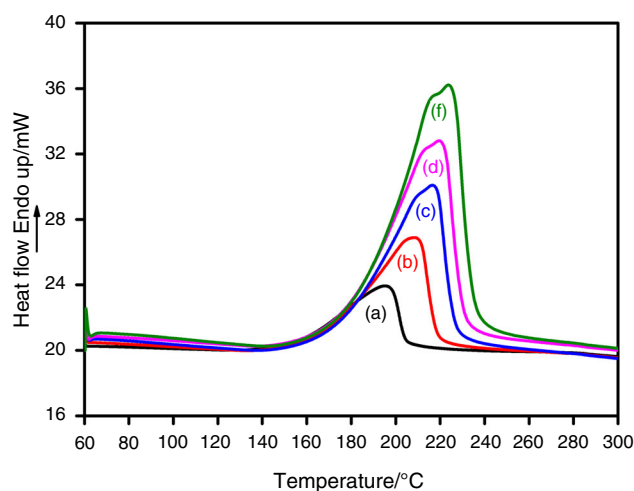
Fig. 5 DSC curves of the synthesized KMnPO$_4$·H$_2$O at different heating rates: 5 (*a*), 10 (*b*), 15 (*c*), 20 (*d*), and 25 (*f*) K min^{-1}

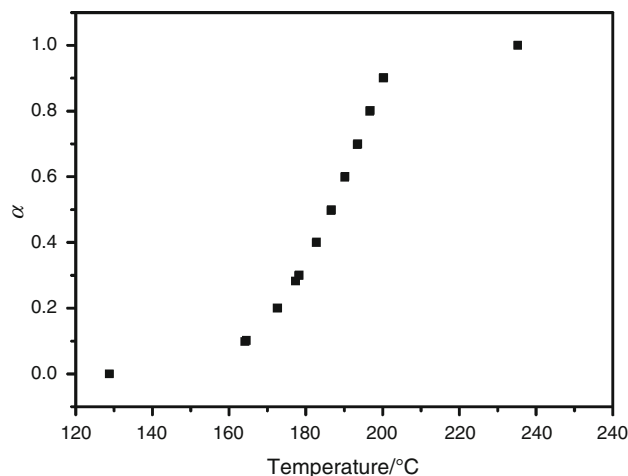**Fig. 3** XRD patterns of the synthesized KMnPO$_4$·H$_2$O (*a*) and standard file PDF#802360 (*b*)

Fig. 6 Degree of conversions α versus *T* for the dehydration of synthesized KMnPO$_4$·H$_2$O at the heating rate of 5 K min^{-1}

Table 1 The peak temperature (T_p) and enthalpy of dehydration of KMnPO$_4$·H$_2$O at various heating rates

Heating rates/K min^{-1}	Peak temperature/K	ΔH/Jg^{-1}
5	468.15	297.29
10	481.27	282.15
15	489.62	289.90
20	493.02	285.35
25	496.85	287.01
Average	485.78	288.34 ± 5.74

apparent activation energies using KAS and iterative KAS equations as mentioned before. Figure 6 indicates the tentative probable mechanism models of the dehydration process to be the types of order-based (F), geometrical contraction (R), and Avrami-Erofeev (A) models [28].

Table 1 illustrates the peak temperature (T_p) and enthalpy changes (ΔH) of the dehydration reaction of KMnPO$_4$·H$_2$O confirm an endothermic process. The results in Table 2 reveal that the activation energy (E_α or E) is approximately independent on alpha (α). In fact, if E values are independent on α, it means that the process is a single-step reaction [29, 30]. Hence, this dehydration process can be interpreted to be the single-step reaction. The iterative procedure was carried out to calculate the apparent E approximating the exact value according to the following equation [31, 32].

$$\ln \frac{\beta}{h(x)T^2} = \ln \frac{AE}{g(\alpha)R} - \frac{E}{RT}, \tag{8}$$

where $x = E/RT$ and $h(x)$ is suggested by the fourth Senum and Yang [33] approximation formulae

$$h(x) = \frac{x^4 + 18x^3 + 86x^2 + 96x}{x^4 + 20x^3 + 120x^2 + 240x + 120}. \tag{9}$$

Based on the data in Fig. 5, the calculated apparent E approximating the exact values at various degrees of conversion α of the dehydration process of KMnPO$_4$·H$_2$O by KAS and iterative methods were evaluated. The results were presented in Fig. 7. The average activation energies from both methods were found to be 101.26 and 101.45 kJ mol^{-1}, respectively. The results agree well with the our previous work [22]. The A values were found to be based on the mechanism function of $g(\alpha) = (1-(1-\alpha)^{2/3})$ or differential form of $f(\alpha) = (3/2)(1-\alpha)^{1/3}$ and having the A values of 2.1481×10^5 (KAS) and 2.4664×10^5 s^{-1} (iterative). These values were obtained by the simple method as well as presented in wide publications [31, 34]. Equation 10 was used to confirm the mechanism function for the single-step reaction. The results are tabulated in Table 3 and confirmed the best mechanism function to be $F_{1/3}$ model, which agree with Fig. 6.

$$\ln g(\alpha) = \left[\ln \frac{AE}{R} + \ln \frac{e^{-x}}{x^2} + \ln h(x)\right] - \ln \beta. \tag{10}$$

According to the mentioned mechanism model including this experimental data, the kinetic equation is suggested to be:

$$1 - (1 - \alpha)^{2/3} = kt. \tag{11}$$

Hence, the differential rate law can be expressed as follows

$$\frac{d\alpha}{dt} = 2.1481 \times 10^5 \times \frac{3}{2}(1-\alpha)^{1/3}e^{-\frac{101.26}{RT}} \text{ (KAS)}. \tag{12}$$

$$\frac{d\alpha}{dt} = 2.4664 \times 10^5 \times \frac{3}{2}(1-\alpha)^{1/3}e^{-\frac{101.45}{RT}} \text{ (iterative KAS)}. \tag{13}$$

Table 2 Activation energy values (E_α), pre-exponential factor (A), and correlation coefficient (r^2) calculated by KAS and iterative methods for the dehydration of KMnPO$_4$·H$_2$O in nitrogen atmosphere

α	KAS method			Iterative method (KAS)		
	E_α/kJ mol^{-1}	r^2	lnA*	E_α/kJ mol^{-1}	r^2	lnA*
0.1	107.16	0.9950	13.6398	107.40	0.9951	13.7689
0.2	102.90	0.9941	12.6629	103.15	0.9941	12.7959
0.3	101.51	0.9930	12.3556	101.77	0.9931	12.4905
0.4	101.19	0.9923	12.2923	101.45	0.9923	12.4290
0.5	100.70	0.9924	12.1733	101.24	0.9925	12.3079
0.6	100.97	0.9919	12.2329	100.37	0.9919	12.3810
0.7	100.09	0.9933	12.0077	100.37	0.9934	12.1486
0.8	99.75	0.9935	11.9090	100.04	0.9936	12.0543
0.9	97.02	0.9966	11.2244	97.31	0.9966	11.3652
Average	101.26 ± 2.73	0.9936	12.2775	101.45 ± 2.74	0.9936	12.4157

* Based on the mechanism function of $F_{1/3}$: $g(\alpha) = (1-(1-\alpha)^{2/3})$
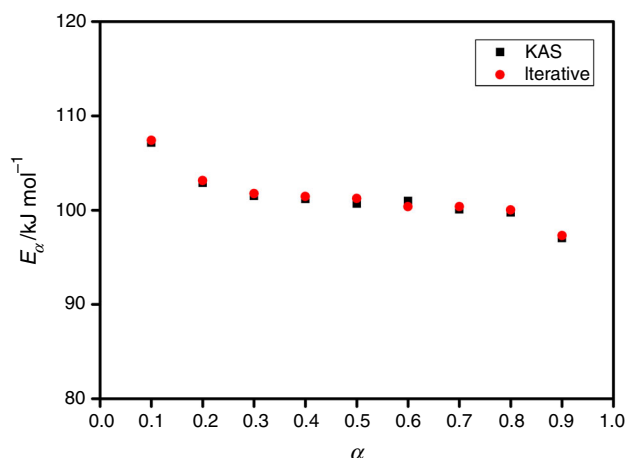
Fig. 7 Dependence of E_α on α ($\alpha = 0.1$–0.9) obtained from KAS and iterative methods

Table 3 The most probable mechanism functions $g(\alpha)$, slopes and the correlation coefficients of linear regression (r^2) calculated from Eq. 10

Temperature/K	Mechanism model	r^2	Slope
463	$F_{1/3}$	0.99748	−1.05375
	$F_{3/4}$	0.99682	−1.14541
	R_1	0.99728	−0.98536
	R_2	0.99734	−1.08958
	A_1	0.99598	−1.20375
	$A_{3/2}$	0.99598	−0.8025
468	$F_{1/3}$	0.99774	−1.00235
	$F_{3/4}$	0.99461	−1.13575
	R_1	0.99872	−0.90671
	R_2	0.99672	−1.05383
	A_1	0.99188	−1.22339
	$A_{3/2}$	0.99188	−0.81559
473	$F_{1/3}$	0.99722	−0.95924
	$F_{3/4}$	0.99192	−1.16519
	R_1	0.99684	−0.82278
	R_2	0.99581	−1.03668
	A_1	0.98621	−1.30914
	$A_{3/2}$	0.98621	−0.87276

Equations 12 and 13 express that the dehydration rate equation. The rate of reaction $\left(\frac{d\alpha}{dt}\right)$ depends on α and T. At a constant degree of conversion α, the reaction rate increases with increasing T. When T is kept constant, then the rate decreases with increasing α values. In the range of $0.1 < \alpha < 0.3$, the effect of T on the rate is dominant, while in the range of $0.3 < \alpha < 0.9$, the value of α is dominant on affecting the rate.

Conclusions

The alternative evaluation methodology by combining the DSC data and the Origin Lab program is presented. This method is suitable for the evaluation of the peak area at a current temperature from DSC data, in the case of the DSC instrument lacks of the internal software for the calculation of the peak area. The title compound was characterized by standard methods and the morphologies were found to be plate-like in micro-scalesize. The kinetic studies of thermal decomposition of the title compound were carried out by KAS and iterative methods. The relationship between the degree of conversions α and temperature supports the most probable mechanism function of type $F_{1/3}$. Complete kinetic study including the exact value of activation energy of $KMnPO_4 \cdot H_2O$ is first reported. Since, the synthesized compound is an alternative precursor for the preparation of $LiMnPO_4$, that used as a cathode in lithium ion batteries. Therefore, the exact kinetic and thermodynamic data obtained from this work are important information for the production process development of $LiMnPO_4$.

References

1. Šoptrajanov B, Stefov V, Kuzmanovski I, Jovanovski G, Lutz HD, Engelen B. Very low H–O–H bending frequencies. IV. Fourier transform infrared spectra of synthetic dittmarite. J Mol Struct. 2002;613:7–14.
2. Lapina LM. Metal ammonium phosphates: new application areas. Usp Khim. 1968;37:693–701.
3. Barros N, Airoldi C, Simoni JA, Ramajo B, Espina A, Garcia JR. Calorimetric determination of the effect of ammonium-iron(II) phosphate monohydrate on *Rhodic Eutrudox* Brazilian Soil. Spectrochim Acta. 2006;441:89–95.
4. Erskine AM, Grim G, Horning SC. Ammonium ferrous phosphate. Ind Eng Chem. 1944;36:456–60.
5. Koleva V, Zhecheva E, Stoyanova R. Facile synthesis of LiMnPO4 olivines with a plate-like morphology from a dittmarite-type $KMnPO_4 \cdot H_2O$ precursor. Dalton Trans. 2011;40:7385–94.
6. He L, Liu X, Zhao Z. Non-isothermal kinetics study on synthesis of LiFePO4 via carbothermal reduction method. Thermochim Acta. 2013;566:298–304.
7. Su J, Wei BQ, Rong JP, Yin WY, Ye ZX, Tian XQ, Ren L, Cao MH, Hu CW. A general solution-chemistry route to the synthesis LiMPO4 (M = Mn, Fe and Co) nanocrystals with [010] orientation for lithium ion batteries. J Solid State Chem. 2011;184:2909–19.
8. Zhang Y, Huo QY, Du P, Wang LZ, Zhang AQ, Song YH, Lv Y, Li GY. Advances in new cathode material LiFePO4 for lithium-ion batteries. Synth Met. 2012;162:1315–26.
9. Xuehang W, Wenwei W, Sen L, Yanjin F, Shushu L. Preparation via solid-state reaction at room temperature and characterization of layered nanocrystalline KMnPO4.H2O. J Alloys Compd. 2009;479:541–4.

10. Koleva VG. Metal-water interactions and hydrogen bonding in dittmarite-typecompounds $M\bullet M''PO_4\cdot H_2O$ ($M\bullet = K^+$, NH_4^+; $M'' = Mn^{2+}$, Co^{2+}, Ni^{2+}): correlations ofIR spectroscopic and structural data. Spectrochim Acta. 2005;Part A 62:1196-1202

11. Visser D, Carling SG, Day P, Deportes J. Magnetic structure of $KMnPO_4\cdot H_2O$. J Appl Phys. 1991;69:6016–8.

12. Ryu SH, Sin JH, Shanmugharaj AM. Study on the effect of hexamethylene diamine functionalized graphene oxide on the curing kinetics of epoxy nanocomposites. Eur Polym J. 2014;52:88–97.

13. Zvetkov VL, Djoumaliisky S, Simeonova-Ivanova E. The non-isothermal DSC kinetics of polyethylene tereftalate–epoxy compatible lends. Thermochim Acta. 2013;553:16–22.

14. Tanwar N, Saraswat VK. A study of kinetics of phase transformation of $Ge_{10}Se_{75}Sb_{15}$ chalcogenide glass. J Non-Cryst Solids. 2014;394–395:1–5.

15. He Y, Liao S, Chen Z, Li Y, Xia Y, Wu W, Li B. Nonisothermal kinetics study with advanced isoconversional procedure and DAEM. J Therm Anal Calorim. 2014;115:237–45.

16. Zvetkov VL, Krastev RK, Samichkov VI. Rate equations in the study of the DSC kinetics of epoxy-amine reactions in an excess of epoxy. Thermochim Acta. 2008;478:17–27.

17. Ručigaj A, Alič B, Krajnc M, Šebenik U. Investigation of cure kinetics in a system with reactant evaporation: epoxidized soybean oil and maleic anhydride case study. Eur Polym J. 2014;52:105–16.

18. Xiao L, Li L, Fu F, He M. Studies on non-isothermal and isothermal dehydration kinetics of $FePO_4\cdot 2H_2O$. Thermochim Acta. 2012;541:57–61.

19. Kissinger HE. Reaction kinetics in differential thermal analysis. Anal Chem. 1957;29:1702–6.

20. Akahira T, Sunose T. Transactions of the 1969 Joint convention of four electrical institutes; Paper No. 246, 1969; Research Report, Chiba Institute of Technology (Sci. Technol.) 1971;16:22–23.

21. Basset H, Bedwell WL. Studies of phosphates. Part I. Ammonium magnesium phosphate and related compounds. J Chem Soc. 1933;137:854–71.

22. Noisong P, Danvirutai C. Kinetics and mechanism of thermal dehydration of $KMnPO_4\cdot H_2O$ in a nitrogen atmosphere. Ind Eng Chem Res. 2010;49:3146–51.

23. Wang W, Gao X, Zheng L, Lan Y. Reductive dechlorination of polychlorinated dibenzo-p-dioxins and dibenzofurans in MSWI Fly ash by sodium hypophosphite. Sep Purif Technol. 2006;52:186–90.

24. Pejov L, Šoptrajanov B, Jovanovski G. Very low H–O–H bending frequencies. II. quantum chemical study of the water bending potential in compounds of the $MKPO_4\cdot H_2O$ types. J Mol Struct. 2001;563–564:321–7.

25. Šoptrajanov B. Very low H–O–H bending frequencies. I. Overview and infrared spectra of $NiKPO4\cdot H2O$ and its deuterated analogues. J Mol Struct. 2000;555:21–30.

26. Šoptrajanov B, Jovanovski G, Pejov L. Very low H–O–H bending frequencies. III. fourier transform infrared study of cobalt potassium phosphate monohydrate and manganese potassium phosphate monohydrate. J Mol Struct. 2002;613:47–54.

27. Falk M. The frequency of the H—O—H bending fundamental in solids and liquids. Spectrochim Acta. 1984;40A:43–8.

28. Khawam A. Flanagan DR, Solid-state kinetic models: basics and mathematical fundamentals. J Phys Chem B. 2006;110:17315–28.

29. Huang Y, Xia Y, Lioa S, Tong Z, Liu G, Li Y, Chen Z. Synthesis of α-Al_2O_3 platelets and kinetics study for thermal decomposition of its precursor in molten salt. Ceram Int. 2014;40:8071–9.

30. Gao X, Dollomore D. The thermal decomposition of oxalates: part 26. A kinetic study of the thermal decomposition of manganese(II) oxalate dehydrate. Thermochim Acta. 1993;215:47–63.

31. Vlaev L, Nedelchev N, Gyurova K, Zagorcheva M. A comparative study of non-isothermal kinetics of decomposition of calcium oxalate monohydrate. J Anal Appl Pyrolysis. 2008;81:253–62.

32. Gao Z, Wang H, Nakada M. Iterative method to improve calculation of the pre-exponential factor for dynamic thermogravimetric analysis measurement. Polymer. 2006;47:1590–6.

33. Senum GI, Yang RT. Rational approximations of the integral of the Arrhenius equation. J Therm Anal Calorim. 1977;11:445–7.

34. Liqing L, Donghua C. Application of iso-temperature method of multiple rate to kinetic :analysis dehydration for calcium oxalate monohydrate. J Therm Anal Calorim. 2004;78:283–93.